International Journal of Pharmaceutics 678 (2025) 125670

Contents lists available at ScienceDirect

International Journal of Pharmaceutics

journal homepage: www.elsevier.com/locate/ijpharm

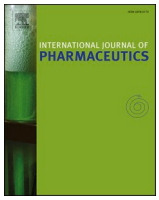

Can bacteriophage be stabilised by lipid encapsulation when nebulised for inhalation delivery against *Pseudomonas aeruginosa*?

Yue Cao [a], Yuncheng Wang [a,b], Mengyu Li [a], Dipesh Khanal [a,*], Hak-Kim Chan [a,*]

[a] Advanced Drug Delivery Group, Sydney Pharmacy School, Faculty of Medicine and Health, The University of Sydney, NSW 2006, Australia
[b] Jiangsu Key Laboratory of Marine Bioresources and Environment, Co-Innovation Center of Jiangsu Marine Bio-industry Technology, Jiangsu Key Laboratory of Marine Pharmaceutical Compound Screening, College of Pharmacy, Jiangsu Ocean University, Lianyungang 222005, China

A B S T R A C T

Inhaled bacteriophage (phage) therapy is emerging as a promising approach to combat multidrug-resistant (MDR) respiratory pathogens such as *Pseudomonas aeruginosa*. Aerosol delivery by nebulization poses challenges for maintaining phage stability, often resulting in titer losses due to mechanical stresses. This study evaluated the use of liposomal encapsulation to protect phages during nebulization. Two *P. aeruginosa* phages, PEV2 (short-tail) and PEV40 (long-tail), were selected for this work. Liposomes were prepared using DSPC, cholesterol, Tween 80, and cationic lipid DOTAP. Encapsulation efficiencies were 78 % for PEV2 and 90 % for PEV40, with mean particle sizes of 300 nm and 650 nm, respectively. Nebulization by jet and vibrating mesh devices showed that the liposome-encapsulated phages were able to preserve viability, with titer losses below 0.4 $\log_{10}$ (PEV40) and 0.07 $\log_{10}$ (PEV2). In contrast, non-encapsulated phages experienced titer reductions of up to 1.23 $\log_{10}$, especially by jet nebulization. Vibrating mesh nebulization generated slightly larger droplets (~5.6 μm) but with better phage recovery (> 90 %) and respirable fractions (> 70 %) for both types of phages encapsulated in liposomes. These results demonstrate that the approach of lipid encapsulation effectively protects phages from mechanical damage during nebulization, maintaining bioactivity for aerosol delivery to enhance the success of inhaled phage therapy.

1. Introduction

Bacteriophages (phages) are viruses that target and destroy bacteria, offering a targeted approach to fight bacterial infections (Abedon et al., 2011; Chanishvili, 2012). Respiratory infections caused by MDR pathogens, such as Pseudomonas aeruginosa, are particularly difficult to treat (Essoh et al., 2013; Saussereau et al., 2014). These bacteria often resist common antibiotics and form biofilms in the respiratory tract, which complicates treatment. Inhaled phage therapy offers a promising approach by delivering phages directly to the lungs and minimizing systemic side effects (Groulx et al., 2016; Le Guellec et al., 2023; Semler et al., 2014). Nebulizers are well-suited for pulmonary phage delivery, allowing direct administration into the lower airways with minimal formulation complexity (Cooper et al., 2014).

However, nebulisation can cause significant damage to biological agents. Nebulization of free endolysins, which are enzymes that degrade bacterial cell walls, resulted in a 50 % loss of activity against *Streptococcus pneumoniae*, highlighting the fragility of protein biologics (Wang et al., 2020). Phages, being predominantly composed of proteins, are potentially at an even greater risk of structural damage during nebulization compared to simpler biological agents. This increased vulnerability stems from their more intricate architecture of the capsid and tail, which are susceptibility to damage by shear forces, cavitation, and exposure to air–liquid interfaces (Carrigy et al., 2017; Liu et al., 2012; Turgeon et al., 2014). Nebulization has been shown to significantly diminish phage titers, potentially compromising their therapeutic efficacy (Astudillo et al., 2018; Carrigy et al., 2017; Le Guellec et al., 2023; Leung et al., 2019). Our previous study revealed varying levels of phage inactivation caused by different nebulizer types: air jet nebulizers induced the greatest damage, with up to 94 % phage inactivation, while vibrating mesh nebulizers resulted in approximately 75 % inactivation Structural alterations including capsid deformation and tail contraction compromise the ability of phages to effectively infect bacterial hosts (Astudillo et al., 2018; Leung et al., 2019). Addressing this stability issue is critical, as a loss of viable phages during aerosol delivery to the lungs could significantly undermine the efficacy and reliability of inhaled phage therapy.

Lipid encapsulation is a promising way to protect and stabilise a range of biological agents, including proteins and nucleic acids (Jiang et al., 2024; Neary et al., 2024). Additionally, phages encapsulated in lipids can penetrate biofilms better or be more effectively taken up by host cells in the lungs where intracellular pathogens may reside, further enhancing their therapeutic potential (Lee et al., 2022; Wang et al., 2019). Nebulizing lipid-based formulations has also shown promising

* Corresponding authors.
E-mail addresses: dipesh.khanal@sydney.edu.au (D. Khanal), kim.chan@sydney.edu.au (H.-K. Chan).

https://doi.org/10.1016/j.ijpharm.2025.125670
Received 20 March 2025; Received in revised form 30 April 2025; Accepted 30 April 2025
Available online 8 May 2025

results in lung delivery, improving deposition, retention, and distribution of therapeutics in the airways (Elhissi, 2017; Rudokas et al., 2016). In our study, we developed a liposomal formulation to stabilize bacteriophages during nebulization. The formulation includes: DOTAP, a model cationic lipid that facilitates binding to the negatively charged phage (Liu et al., 2024); cholesterol, which maintains the integrity of the lipid bilayer (Szabová, 2021); DSPC, a saturated phospholipid that provides resistance against shear forces (Anderson and Omri, 2004); and Tween 80, a non-ionic surfactant that forms a protective foam to cushion the phage (Israelachvili, 2011). These components were carefully selected to address the challenges of nebulization.

To date, while most existing studies have focused on the nebulization of free phages, none have examined lipid encapsulation as a protective measure for phages during aerosolization. In this study, we assessed the viability and structural integrity of lipid-encapsulated phages post-nebulization. By demonstrating a stable and effective liposomal phage delivery system, this approach could pave the way for more effective inhaled phage therapy to tackle the growing challenge of antibiotic resistance in respiratory infections.

2. Materials and methods

Bacteriophages

Two types of *Pseudomonas* lytic phage, a podovirus (PEV2, short-tailed) and a myovirus (PEV40, long-tailed) were originally isolated from the sewage treatment plant in Olympia (WA, USA) by the Kutter Lab (Evergreen Phage Lab). Phage isolation utilized *Pseudomonas aeruginosa* dog-ear strain PAV237, which also served as the host for amplification and titer assessment (plaque assay). Phage purification was conducted as described in our previous study (Cao et al., 2023). Briefly, 30 mL of each amplified phages were filtered using a 0.22 μm PES syringe filter, treated with 10 μg/mL DNase and RNase at 37 °C for 30 min, and purified via ultrafiltration at 4000 × g at 4 °C. Samples were resuspended in phosphate buffered saline (PBS) at pH 7.2, and endotoxins removed with EndoTrap®HD prior to anion-exchange (AEX) chromatography using a CIMmultus™ DEAE column. Phages were eluted with NaCl buffers optimized for purity, followed by endotoxin cleanup with EndoTrap®HD. Endotoxin levels were quantified with the ToxinSensor™ LAL assay, and purified phages PEV2 and PEV40 (1 x 10^{10} pfu/mL) were stored in PBS.

Lipid encapsulated phages

A mixture of 1,2-distearoyl-*sn*-glycero-3-phosphocholine (DSPC), cholesterol, Tween 80, and 1,2-dioleoyl-3-trimethylammonium propane (DOTAP) at molar ratio of 7:3:1:2 was dissolved in absolute ethanol with a total solid content of 20 mg/mL. The solution was bath-sonicated for 10 min under ambient condition. For lipid-encapsulated phage preparation, a confined impinging jet mixer (CIJ)—previously previously described for nanoparticle synthesis (Chiou et al., 2008)—was employed. The lipid mixture was injected into one inlet channel of the CIJ, while the phage suspension was introduced into the second inlet channel. The resulting liposome was collected via the outlet tube into a scintillation vial. The total flow rate (TFR) was maintained at 17.5 mL/min with fixed flow rate ratio (FRR) of 1:1 between lipid stream and aqueous (phage) stream. Empty liposome (control) was produced by only introducing PBS into the second inlet channel. All experiments were conducted at room temperature and triplicated.

Ethanol removal

Ethanol-free liposome-phage suspensions were obtained by ultracentrifugation at 10000x*g* for 30 min at 4 °C. The supernatant was decanted, and the pellet was resuspended in PBS. This process was repeated two times to minimise residual ethanol content.

Liposomal size measurement

The size and PDI of the liposomes were measured using dynamic light scattering (DLS) on a Zetasizer Nano-ZS (Malvern Instruments, UK) with a 633 nm He/Ne laser and 4.0 mW power to report the intensity mean diameter (Z-average). Liposomal phage suspensions were diluted 1:10 in PBS for analysis of size distribution. Measurements were conducted in triplicate at 25 °C.

Zeta potential

The zeta potential of liposomes was measured by Laser Doppler Electrophoresis using the Zetasizer Nano ZS (Malvern Instruments, UK) and calculated with the Helmholtz-Smoluchowski equation. Samples were diluted in PBS to a lipid concentration of 0.2 mg/mL and analyzed in a folded capillary cell. Measurements were performed in triplicate at 25 °C.

Transmission electron microscopy (TEM)

Morphology and structure of phage-loaded liposomes before and after nebulisation were examined by transmission electron microscopy (TEM). Similar to our previous protocol (Cao et al., 2023), we employed an FEI Tecnai T12 microscope (FEI, USA) with a 4 k × 4 k CCD camera. Samples were negatively stained on glow-discharged carbon-coated copper grids (GSCU150CC-50, Proscitech, Australia) to reduce hydrophobicity. For staining, 10 μL drops of the sample, 2 % w/v uranyl acetate, and Milli-Q water were placed on parafilm. Grids were immersed in the sample for 2 min, blotted, stained for 10 sec, rinsed in water for 10 sec, and air-dried for 3 min before imaging.

Plaque assay

The Miles-Misra surface droplet technique (Carlson, 2005) was used to quantify viable phages in original and lysed liposome samples before and after nebulisation. Serial 1:10 dilutions were prepared by mixing 20 μL of the sample with 180 μL PBS. A suspension of ~2 × 10^9 CFU host bacteria in 5 mL molten soft agar (0.4 % Amyl agar, 48 °C) was overlaid onto a nutrient agar plate (1.5 % Amyl agar and nutrient broth). Diluted phage samples (10 μL) were spotted onto the agar in triplicate, air-dried, and incubated at 37 °C overnight. Plaques within the number range of 3–30 were counted to calculate phage viability.

The encapsulation efficiency of the phages

Phage encapsulation efficiency (EE) was calculated using the formula: $EE\ (\%) = 100 - (C_{free}/C_{total}) \times 100$, where C_{total} is the total phage titer, and C_{free} is the free phage concentration. C_{free} was measured via plaque assay on the liposome-encapsulated phage suspension, while C_{total} was determined by lysing 0.5 mL of the suspension with 0.5 mL bile salts (Sigma-Aldrich, NSW, Australia) (50 mM) before the plaque assay. Control tests confirmed that this bile salt concentration did not affect phage infectivity across titers ranging from 10^1 to 10^{10} pfu/mL.

Phage nebulisation

A 3 mL phage stock (free phage or liposome encapsulated phage) suspension was nebulized using two types of nebulizers: a jet nebulizer (PARI LC Sprint, Pari Respiratory Equipment, USA) and a vibrating mesh nebulizer (eFlow Rapid, Pari Respiratory Equipment, USA). Nebulized aerosols were collected using a method adapted from our previous studies (Astudillo et al., 2018; Cipolla, 1994) designed for nebulized protein collection (Fig. 1). The aerosol was drawn into an ice-cooled test tube inside an aspiration flask via Tygon tubing connected to a 2.0 mL plastic pipette, operating at 8 L/min. For the mesh nebulizers, the apparatus functioned without compressed air. Samples collected in the test tube were analyzed via TEM and plaque assay. All nebulization runs were performed in triplicate. Aerosol collection efficiency was assessed by the volume recovered in the test tube, with aerosols deposited in tubing washed and included. Recovery was $\geq$ 80 % for the air-jet nebulizer and $\geq$ 90 % for the mesh nebulizers. The lower efficiency of the air-jet nebulizer was attributed to fine aerosol droplets escaping in the airstream. Despite this, the apparatus effectively captured the majority of aerosols generated by all nebulizers.

Statistical analysis

Statistical analysis was conducted using one-way analysis of variance (ANOVA) and unpaired two-sample t-tests at a 95 % confidence level to assess differences in liposome size, zeta potential, titer reduction, and encapsulation efficiency. Statistical significance was determined for p values < 0.05.

Aerosol droplet size distribution

To assess the particle size distribution (PSD) of nebulized phage

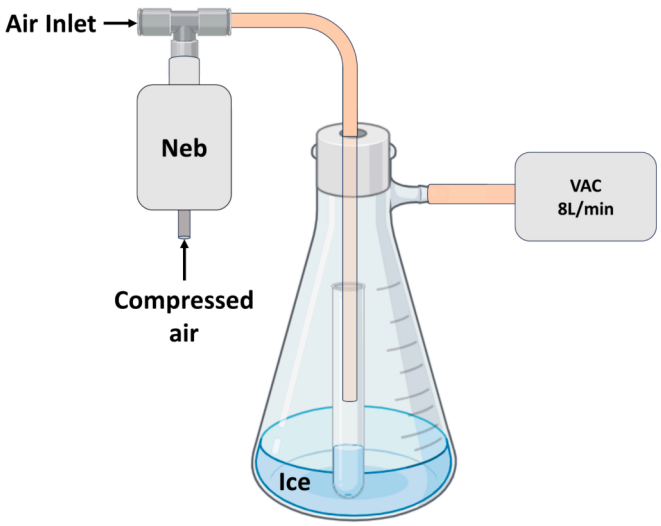

Fig. 1. Apparatus for trapping nebulized liposome-encapsulated and non-encapsulated phages from nebulizers.

aerosols produced from the nebulizer devices, laser diffraction was employed using a Spraytec system (Malvern Instruments Ltd., UK). We conducted continuous nebulization for 60 s, taking measurements at one-second intervals. The data was then analyzed to determine the median diameter (D50) and span. The span was calculated using the formula (D90 − D10)/D50, where D10, D50, and D90 represent the particle diameters at the 10th, 50th, and 90th percentiles of the distribution, respectively.

Viable phage respirable fraction

A multi-stage liquid impinger (MSLI, Copley, Nottingham, UK) running at 30 L/min was used to measure the total viable phage in aerosol droplets (≤4.5 μm) (Astudillo et al., 2018). The MSLI stages had cut-off diameters of 16.9 μm (stage 1), 9.3 μm (stage 2), 4.5 μm (stage 3), and 2.5 μm (stage 4), with the filter (stage 5) collecting particles < 2.5 μm. During measurement, each impinger stage was pre-filled with 10 mL PBS, and the nebulizer was connected to the MSLI using a silicone adapter and a United States Pharmacopeia (USP) induction port. A 3 mL phage suspension was nebulized into the MSLI, and the adapter, USP throat, and filter stage were washed separately with 10 mL PBS to ensure complete recovery. Viable phages at each stage were quantified using plaque assays. The titers from stage 3, 4 and the filter stage were summed to determine the viable phage content in the respirable fraction (RF). The viable respirable fraction (VRF) was defined as the titers recovered from these two stages relative to the total titer initially loaded into the nebulizer. The titers of liposome encapsulated phages were determined by plaque assay after complete liposome lysis with 50 mM bile salts.

3. Results

Characteristics of phage-encapsulated liposomes.

Phage viability and encapsulation efficiency

Table 1
Characterization of free form, pure liposome and liposome encapsulating PEV2 and PEV40 (Size (z-average), polydispersity index (PDI), zeta potential and encapsulation efficiency (EE%).

Phage type	Size (nm)	PDI	Zeta potential(mV)	EE(%)
PEV2	70.2 ± 2.73	0.11 ± 0.03	−19.3 ± 3.03	N/A
PEV40	185 ± 6.94	0.19 ± 0.03	−25.5 ± 2.22	
Pure liposome	89.3 ± 5.8	0.18 ± 0.02	42.5 ± 1.2	
Lipo_PEV2	301 ± 35.8	0.55 ± 0.04	0.17 ± 0.04	77.9 ± 1.48
Lipo_PEV40	651 ± 14.3	0.79 ± 0.07	0.90 ± 0.72	83.9 ± 4.23

The encapsulation efficiencies for PEV2 and PEV40 produced by the CIJ mixer were 77.9 ± 1.48 %, 83.9 ± 4.23 %, respectively (Table 1).

Liposomal size distribution and zeta potential

The liposomes entrapping short-tail phage PEV2 averaged 301 ± 35.8 nm with a polydispersity index (PDI) of 0.28 ± 0.06, while those encapsulating long-tail phage PEV40 were larger at 651 ± 14.3 nm with a PDI of 0.37 ± 0.12 (Table 1.). The z-average values were 70.2 ± 2.73 for PEV2, and 185 ± 6.94 for PEV40. The surface charges of the phage-encapsulated liposomes were near-neutral, with zeta potentials of 0.17 ± 0.04 (encapsulated PEV2) and 0.90 ± 0.72 (encapsulated PEV40). In contrast, free phages showed negative zeta potentials of −19.3 ± 3.03 (PEV2) and −25.5 ± 2.22 (PEV40) (Table 1.).

Phage morphology

Fig. 2 illustrates the intact and damaged morphologies of the phages. PEV2 had a short, non-contractile tail (~10 nm) and a ~ 60 nm icosahedral head, while PEV40 possessed a contractile tail (~140 nm) with a similarly sized head (~60 nm). Encapsulated phages were shown located within the larger size white vesicles along with smaller empty liposomes nearby.

Effect of nebulisation

Titer reduction

Phage viability analysis (determined by plaque assay after complete liposome lysis with 50 mM bile salts) (Fig. 3) showed that non-encapsulated PEV40 experienced mild titer loss of 0.67 $\log_{10}$ in the vibrating mesh nebulization process, but it was substantially inactivated in the air jet nebulization (1.23 $\log_{10}$ titer loss). In contrast, liposome-encapsulated PEV40 remained practically unaffected by both nebulization processes, with titer loss being less than 0.4 $\log_{10}$. Similarly, for liposome-encapsulated PEV2, both types of nebulizers had a negligible effect with titer reduction of < 0.07 $\log_{10}$. Like PEV40, non-encapsulated PEV2 was significantly inactivated (1.1 $\log_{10}$ titer loss) by jet nebulization, but with only little titer loss by vibrating mesh nebulization (~0.26 $\log_{10}$).

Particle size distribution of nebulised aerosols

The geometrical sizes of aerosols generated by the two nebulizers are shown in Table 2. The D_{50} of liposome-encapsulated PEV2 and PEV40 droplets produced by the jet nebulizer were 3.10 ± 0.05 μm and 2.98 ± 0.04 μm, respectively. The vibrating mesh nebulizer generated larger droplets of liposomal PEV2 (5.60 ± 0.13 μm) and PEV40 (5.83 ± 0.21 μm), which are still suitable for inhalation (Astudillo et al., 2018).

***In vitro* aerosolization performance**

The deposition profiles, recovery, and VRF from the two nebulizers are shown in Fig. 4. At the same loading volume (3 mL suspension sample), the amount of viable encapsulated phages retained in the device was lower in the vibrating mesh nebulizer than with the jet nebulizer. The vibrating mesh-nebulized aerosols had significantly higher deposition at the lower stages (stage 2–4 and filter) of the impactor, compared with the jet-nebulized ones. As a result, the vibrating mesh nebulizer demonstrated superior performance, yielding high recoveries for both PEV2 (94.3 ± 3.60 %) and PEV40 (96.2 ± 2.34 %). In comparison, the jet nebulizer showed comparable recovery for PEV2(95.1 ± 3.65 %) but significantly lower recovery for PEV40 (48.9 ± 0.84 %). Regarding the VRF, which indicates the proportion of phages likely to reach the deep lungs, the vibrating mesh nebulizer produced 70.3 ± 1.78 % (PEV2) and 74.8 ± 1.96 % (PEV40), which are substantially higher than those from the jet nebulizer, 44.0 ± 2.6 % (PEV2) and (28.2 ± 0.99 % (PEV40).

4. Discussion

Our study examined the potential of liposomal encapsulation to overcome phage inactivation during nebulization for pulmonary delivery. We investigated two *P. aeruginosa* phages with distinct morphologies: PEV2 (a short-tailed podovirus) and PEV40 (a long-tailed myovirus). The results demonstrated that liposome encapsulation effectively protected both types of phage during jet and vibrating mesh

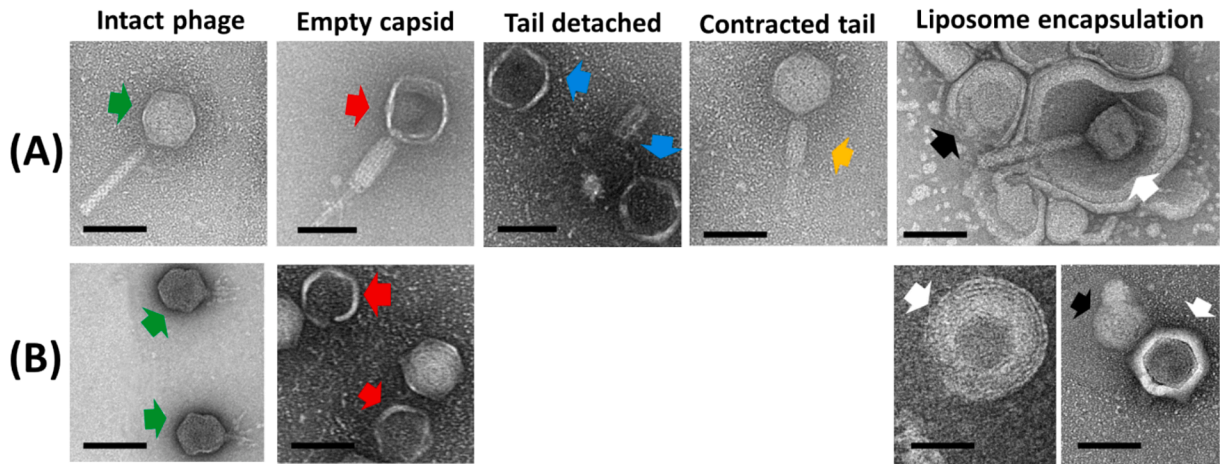

Fig. 2. TEM images of (A) PEV40 and (B) PEV2 phages. Green arrows indicate intact phages, red arrows empty capsids, blue arrows detached tails, and orange arrows contracted tails. White arrows mark lipid-encapsulated phages and black arrows empty liposomes appear. (Scale bar: 100 nm).

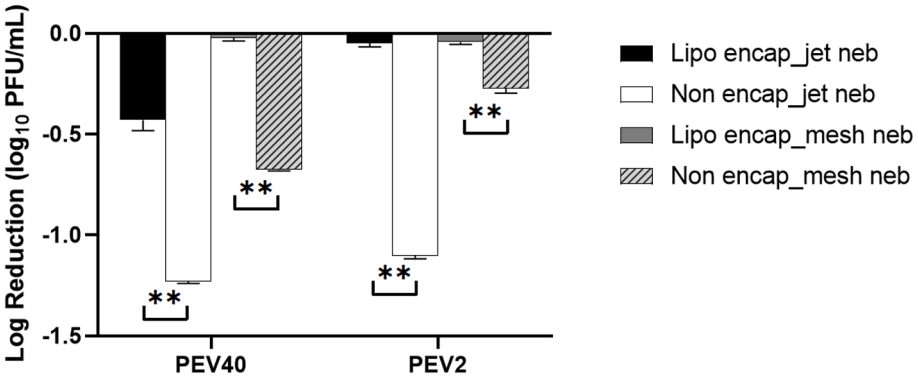

Fig. 3. Comparison of liposome encapsulated and non-encapsulated phage deactivation after nebulization. Phage titers were determined by plaque assay on P. aeruginosa (strain PAV237, see Methods) after complete liposome lysis with 50 mM bile salts. Error bars for the plaque assay represent one standard deviation of triplicate experiments. Double asterisk (**) denotes a statistically significant difference with $p < 0.01$.

Table 2
Geometrical size of droplets generated by the two nebulizers.

Nebulisers	Encapsulated samples	D_{10} (μm)	D_{50} (μm)	D_{90} (μm)	Span
Air-Jet	Lipo_PEV2	1.29 ± 0.01	3.10 ± 0.05	7.61 ± 0.20	7.61 ± 0.20
	Lipo_PEV40	1.27 ± 0.0.2	2.98 ± 0.04	7.08 ± 0.21	1.95 ± 0.05
Vibrating mesh	Lipo_PEV2	3.08 ± 0.08	5.60 ± 0.13	10.43 ± 0.54	1.31 ± 0.07
	Lipo_PEV40	3.11 ± 0.08	5.83 ± 0.21	11.23 ± 0.74	1.39 ± 0.06

*Results are average values of triplication measurement. Variations between the three measurements are ≤ 5 %

nebulization, maintaining their viability while producing aerosols suitable for pulmonary delivery. This approach addresses the critical challenge of preserving phage infectivity during the aerosolization process, a key hurdle in developing inhaled phage therapies.

Liposome-encapsulated Phage Formulation. We first achieved reasonably high encapsulation efficiencies of approximately 80 % for PEV2 and 90 % for PEV40 using the CIJ mixing method. TEM images (Fig. 2) confirmed that each phage particle was encapsulated within a larger liposome. The liposome-encapsulated PEV2 had a smaller mean diameter (~300 nm) compared to PEV40 (~650 nm), reflecting their structural differences in tail length (Table 1.). The shift from negative to near-neutral zeta potentials is consistent with the shielding of the negative charge of the phages inside liposomes due to effective phage–lipid interactions, further supporting successful encapsulation of phages into the liposomal structure.

Comparison of Titre Reduction: Encapsulated vs. Free Phages. Notably, titer reductions for liposome-encapsulated phages (deteremined post lysing of liposomes) were minimal after each kind of nebulization, with < 0.07 $\log_{10}$ for PEV2 and < 0.4 $\log_{10}$ for PEV40, even in the high-shear environment of the jet nebulizer. In contrast, biological assays revealed that non-encapsulated phages experienced moderate titer reductions under vibrating mesh nebulization, but significant losses following jet nebulisation (up to 1.23 $\log_{10}$ loss) (Fig. 3). TEM images (Fig. 2) corroborated these findings, showing different morphological alterations in non-encapsulated phages after nebulization, including capsid damage, tail detachment, and tail contraction in these unprotected phages. These results are consistent with our previous findings that phage structure and nebulization method play critical roles in infectivity loss (Carrigy et al., 2017; Cipolla et al., 2014; Fister et al., 2016). Liposomal encapsulation could effectively protect the vulnerable structures of phages against mechanical damage during nebulization.

Analysis of Protective Mechanism. Our liposome formulation is composed of DSPC, cholesterol, DOTAP and Tween 80 (molar ratio 7:3:2:1). The lipid bilayer acts as a protective shell, which buffers the mechanical forces that would otherwise directly impact on the phage structure. This protection mechanism can be understood by interpreting

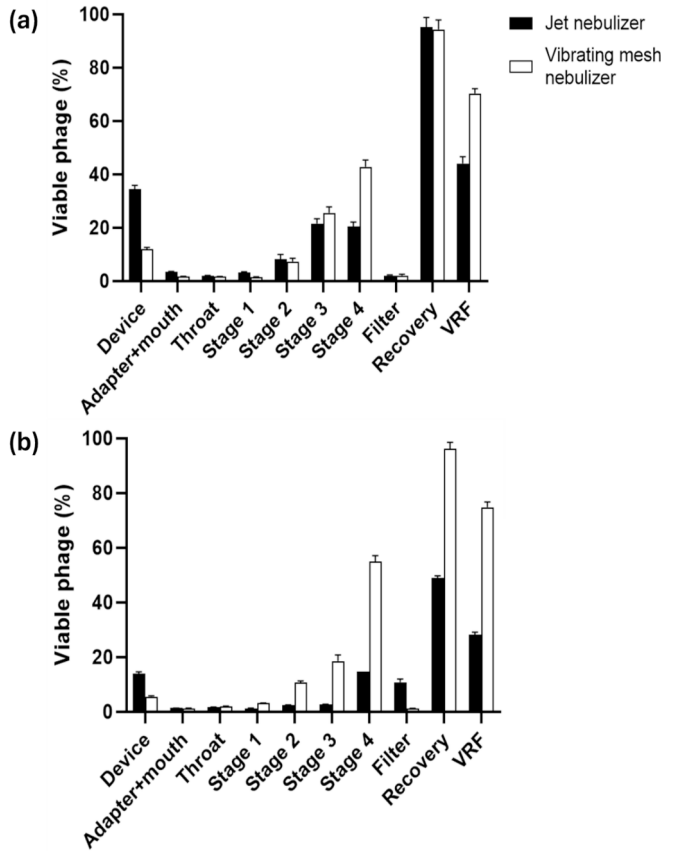

Fig. 4. Titre assay (after complete liposome lysis with 50 mM bile salts) of (a) liposome encapsulated PEV2 and (b) liposome encapsulated PEV40 following *in vitro* deposition of aerosols by the MSLI (n = 3).

the role of each component and comparing our approach to existing literature on liposome stability during nebulization.

DSPC, a saturated phospholipid with a relatively high phase transition temperature (~55 °C), that exceeds physiological conditions, combined with cholesterol, provides structural rigidity to the liposome bilayer. This enhanced rigidity improves resistance against mechanical disruption inherent to pressurized airflow and droplet formation during atomization (Anderson and Omri, 2004; Briuglia et al., 2015). The importance of cholesterol in preserving membrane properties of liposomes during nebulization has been well-documented. Szabová et al. (2021) demonstrated that plain DPPC liposomes lacking cholesterol broke apart under vibrating mesh nebulization and then re-aggregated into larger vesicles with high polydispersity, as evidenced by the zeta potential having shifted from positive to negative values. Incorporating cholesterol (20–40 mol%) significantly improved membrane rigidity, preserving the original size distribution even after nebulization (Szabová, 2021). Several studies suggested at least 30 mol% is usually required to minimize liposomes from content leakage (Briuglia et al., 2015; Soto-Arriaza et al., 2013). However, our formulation achieves stability with a slightly lower cholesterol content (~23 mol% of total lipids), which is likely due to the high proportion of DSPC in keeping the membrane rigidity (Hac-Wydro, 2009). Although cholesterol-free formulations were not directly compared in this study, our choice to include cholesterol was informed by strong evidence from prior literature supporting its stabilizing effect on liposomal membranes during nebulization. Future studies will experimentally validate this by directly comparing DSPC-only liposomes to DSPC:cholesterol formulations under nebulization conditions.

In our formulation, we use the DOTAP to promote the phages entrapment within vesicles (Cuervo et al., 2019; Nap et al., 2014). Additionally, DOTAP may improve liposome vesicle stability by inducing electrostatic repulsion between liposomes and minimising aggregation during nebulization. Tween 80 as a non-ionic surfactant which by reducing surface tension at air–liquid interfaces (Montefusco-Pereira, 2023; Tai et al., 2017), inhibiting excessive vesicle aggregation (Hertel et al., 2015). Additionally, Tween 80 form a foaming layer during nebulization, potentially cushioning liposomes and by adsorbing and dissipating the mechanical stress (Israelachvili, 2011; Rosen, 2004).

Similar strategies have also been employed to preserve the aerosol stability of numerous drugs and biologics with promising outcomes (Ehsan and Clancy, 2015; Lokugamage et al., 2021), with the impact of lipid composition on liposome performance comprehensively reported (Anderson and Omri, 2004; Briuglia et al., 2015; Szabová, 2021). Our results align with these approaches, emphasizing that careful optimization of lipid compositions and stabilizers like Tween 80 can protect phages against the mechanical insults of nebulization, thereby preserving infectivity.

Aerosolization Characteristics. The particle sizing data (Table 1.) indicate that most droplets were under 5 μm, which are suitable for lung delivery. Both liposome-encapsulated PEV2 and PEV40 phages maintained their final titers of approximately 10^9 PFU/mL post-nebulization, a concentration shown to control *P. aeruginosa* infections in animal models (Debarbieux, 2010; Morello et al., 2011).

In Vitro Aerosolization Performance. The respirable fraction of viable phages was measured using MSLI at a flow rate 30 L/min. The jet nebulizer produced lower values of VRF (28.15 ± 0.99 %) and recovery (48.89 ± 0.84 %) for PEV40 compared with PEV2 (VRF 44.03 ± 2.60 % and > 90 % recovery) (Fig. 4). The vibrating mesh nebulizer achieved significantly higher VRF values (>70 %) for both encapsulated phage types with a high viable phage recovery (>90 %), which are most likely attributed to the milder mechanical stress to the phages during operation. Jet nebulization, which uses a high-velocity gas stream to atomize the liposomal-phage suspension into droplets which repeatedly impact on a baffle system, typically subjects particles to intense mechanical stress and air–liquid interfaces. Vibrating mesh nebulizers operate by pushing the liposomal-phage suspension through a mesh (containing ~1000 micro-sized apertures of ~3 μm) via piezoelectric vibration, generally considered a gentler process (Carrigy et al., 2017). Our liposomal formulation demonstrated robust protection in both nebulization systems, regardless of their distinctly different atomization mechanisms, thus broadening the range of nebulizer devices to be used for inhaled phage therapy. This is particularly noteworthy in view of the mixed findings in the literature: while mesh nebulization is generally shown to be less damaging to phages than jet nebulization (Astudillo et al., 2018; Carrigy et al., 2017; Leung et al., 2019), contradictory findings have also been reported (Flint et al., 2023). The consistency of the liposome formulation in maintaining the bioactivity of phages is clinically valuable, as it accommodates variability in clinical equipment and patient-specific delivery requirements (Ari, 2014). When compared to the low VRF values (<15 %) observed in nebulizing free phages (Astudillo et al., 2018), the high VRF values of our liposomal formulations show they can significantly improve delivery to the lungs.

Potential Applications and Future Directions. The use of nebulized liposomal phages provides potential strategies for addressing intracellular infections and biofilm-related complications in respiratory infection. Although phages readily target planktonic bacteria, they often struggle to penetrate host cell membranes and dense biofilm matrices (Chang et al., 2018; Yan et al., 2021). Liposome carriers may enhance the uptake of phages into infected human cells (e.g., through endocytosis) and facilitate their penetration into bacterial biofilms, subsequently releasing the phages to lyse bacterial cells. (Abed and Couvreur, 2014; Ahsan et al., 2024; Meers et al., 2008). The dual capability of enabling targeted delivery to infection sites while maintaining therapeutic titers during aerosolization, positions nebulized liposome-phage formulations as a viable strategy for chronic lung infections (Chan et al., 2014).

Although we focused on two kinds of *P. aeruginosa* phages, the same approach could be adapted for other phage families. Moving towards clinical application in the future will require data on *in vivo* efficacy, pharmacokinetics, and immune responses of repeated phage-liposome doses (Ahsan et al., 2024; Lee et al., 2022; Malik et al., 2017).

5. Conclusion

Lipid-based encapsulation using DSPC, cholesterol, Tween 80, and DOTAP effectively protected phages during nebulization, addressing a critical challenge in inhaled phage therapy. We reached reasonably high encapsulation efficiencies (77.9 % for short-tail PEV2 and 89.93 % for long-tail PEV40) of phages in the lipids, which helped preserve phage structure and viability in both jet and vibrating mesh nebulization. Encapsulated PEV2 and PEV40 showed negligible titer reduction (<0.4 $\log_{10}$), whereas free phages suffered significant inactivation (highest titer loss at 1.23 $\log_{10}$). The vibrating mesh nebulization achieved higher phage recovery (~95 %) and a respirable fraction of ~ 70–75 % for both PEV2 and PEV40 phages, which are desirable for lung deposition. These findings highlight how carefully optimized liposome encapsulation enhances phage stability and delivery to the lungs, thereby offering a promising approach for inhaled phage therapy against MDR pathogens and broadening therapeutic possibilities for challenging pulmonary diseases, including those complicated by biofilm formation.

CRediT authorship contribution statement

Yue Cao: Writing – review & editing, Writing – original draft, Methodology, Investigation, Conceptualization. **Yuncheng Wang:** Writing – review & editing, Methodology, Investigation. **Mengyu Li:** Writing – review & editing, Methodology, Investigation. **Dipesh Khanal:** Writing – review & editing, Supervision, Investigation. **Hak-Kim Chan:** Writing – review & editing, Supervision, Funding acquisition, Conceptualization.

Declaration of competing interest

The authors declare the following financial interests/personal relationships which may be considered as potential competing interests: The authors Y.C. and H-K.C declare that provisional patent applications (Australian Provisional Patent Application Nos. 2024904016 and 2025900910, which are cognate) have been filed in relation to the liposomal encapsulating bacteriophage method described in this manuscript. Apart from these patent applications, no other competing interests exist..

Acknowledgement

This work was supported part by an ARC Discovery Project 210102526 to HKC. The authors thank Dr. Sandra Morales for her generous support of our phage research; Dr. Elizabeth Kutter from the Evergreen Phage Lab, Washington, USA, for providing the phage stocks. The authors acknowledge the facilities and the scientific and technical assistance of Sydney Microscopy & Microanalysis, a core research facility at The University of Sydney. The graphical abstract was created using BioRender.

Appendix A. Supplementary material

Supplementary data to this article can be found online at https://doi.org/10.1016/j.ijpharm.2025.125670.

Data availability

Data will be made available on request.

References

Abed, N., Couvreur, P., 2014. Nanocarriers for antibiotics: a promising solution to treat intracellular bacterial infections. Int. J. Antimicrob. Agents 43, 485-496.http://10.1016/j.ijantimicag.2014.02.009.

Abedon, S.T., Kuhl, S.J., Blasdel, B.G., Kutter, E.M., 2011. Phage treatment of human infections. Bacteriophage 1, 66–85. https://doi.org/10.4161/bact.1.2.15845.

Ahsan, A., Thomas, N., Barnes, T.J., Subramaniam, S., Loh, T.C., Joyce, P., Prestidge, C. A., 2024. Lipid Nanocarriers-enabled delivery of antibiotics and antimicrobial adjuvants to overcome bacterial biofilms. Pharmaceutics 16, 10.3390/pharmaceutics16030396.

Anderson, M., Omri, A., 2004. The effect of different lipid components on the in vitro stability and release kinetics of liposome formulations. Drug Deliv 11, 33-39. http://10.1080/10717540490265243.

Ari, A., 2014. Jet, ultrasonic, and mesh nebulizers: an evaluation of nebulizers for better clinical outcomes. Eurasian J. Pulmonol. 16, 1–7.

Astudillo, A., Leung, S.S.Y., Kutter, E., Morales, S., Chan, H.K., 2018. Nebulization effects on structural stability of bacteriophage PEV 44. Eur. J. Pharm. Biopharm. 125, 124–130. http://10.1016/j.ejpb.2018.01.010.

Briuglia, M.L., Rotella, C., McFarlane, A., Lamprou, D.A., 2015. Influence of cholesterol on liposome stability and on in vitro drug release. Drug Deliv Transl. Res. 5, 231–242. https://doi.org/10.1007/s13346-015-0220-8.

Cao, Y., Khanal, D., Kim, J., Chang, R.Y.K., Byun, A.S., Morales, S., Banaszak Holl, M.M., Chan, H.K., 2023. Stability of bacteriophages in organic solvents for formulations. Int. J. Pharm. 646, 123505.http:// 10.1016/j.ijpharm.2023.123505.

Carlson, K., 2005. Working with bacteriophages: common techniques and methodological approaches. Bacteriophages: Biol. Appl. 1, 437–494.

Carrigy, N.B., Chang, R.Y., Leung, S.S.Y., Harrison, M., Petrova, Z., Pope, W.H., Hatfull, G.F., Britton, W.J., Chan, H.K., Sauvageau, D., Finlay, W.H., Vehring, R., 2017. Anti-Tuberculosis bacteriophage D29 delivery with a vibrating mesh nebulizer, jet nebulizer, and soft mist inhaler. Pharm. Res. 34, 2084–2096. https://doi.org/10.1007/s11095-017-2213-4.

Chan, J.G., Wong, J., Zhou, Q.T., Leung, S.S., Chan, H.K., 2014. Advances in device and formulation technologies for pulmonary drug delivery. AAPS PharmSciTech 15, 882-897. http://10.1208/s12249-014-0114-y.

Chang, R.Y.K., Wallin, M., Lin, Y., Leung, S.S.Y., Wang, H., Morales, S., Chan, H.K., 2018. Phage therapy for respiratory infections. Adv. Drug Deliv. Rev. 133, 76-86. http://10.1016/j.addr.2018.08.001.

Chanishvili, N., 2012. Phage therapy—history from Twort and d'Herelle through soviet experience to current approaches. Adv. Virus Res. 83, 3–40. https://doi.org/10.1016/B978-0-12-394438-2.00001-3.

Chiou, H., Chan, H.K., Prud'homme, R.K., Raper, J.A., 2008. Evaluation on the use of confined liquid impinging jets for the synthesis of nanodrug particles. Drug Dev. Ind. Pharm. 34, 59–64. http://10.1080/03639040701508011.

Cipolla, D., Shekunov, B., Blanchard, J., Hickey, A., 2014. Lipid-based carriers for pulmonary products: preclinical development and case studies in humans. Adv. Drug. Deliv. Rev. 75, 53–80. http://10.1016/j.addr.2014.05.001.

Cipolla, D.C.G., I., 1994. Method for collection of nebulized proteins, in formulation and delivery of proteins and peptides. Am. Chem. Soc. 343–352.

Cooper, C.J., Denyer, S.P., Maillard, J.Y., 2014. Stability and purity of a bacteriophage cocktail preparation for nebulizer delivery. Lett. Appl. Microbiol. 58, 118–122. http://10.1111/lam.12161.

Cuervo, A., Fabrega-Ferrer, M., Machon, C., Conesa, J.J., Fernandez, F.J., Perez-Luque, R., Perez-Ruiz, M., Pous, J., Vega, M.C., Carrascosa, J.L., Coll, M., 2019. Structures of T7 bacteriophage portal and tail suggest a viral DNA retention and ejection mechanism. Nat. Commun. 10, 3746. https://doi.org/10.1038/s41467-019-11705-9.

Debarbieux, L.L., D., Maura, D., Morello, E., Criscuolo, A., Grossi, O., Balloy, V., Touqui, L., 2010. Bacteriophages can treat and prevent Pseudomonas aeruginosa lung infections. J. Infect. Dis. 201, 1096-1104. http://10.1086/651135.

Ehsan, Z., Clancy, J.P., 2015. Management of Pseudomonas aeruginosa infection in cystic fibrosis patients using inhaled antibiotics with a focus on nebulized liposomal amikacin. Future Microbiol. 10, 1901–1912. https://doi.org/10.2217/fmb.15.117.

Elhissi, A., 2017. Liposomes for pulmonary drug delivery: the role of formulation and inhalation device design. Curr. Pharm. Des. 23, 362–372. https://doi.org/10.2174/1381612823666161116114732.

Essoh, C., Blouin, Y., Loukou, G., Cablanmian, A., Lathro, S., Kutter, E., Thien, H.V., Vergnaud, G., Pourcel, C., 2013. The susceptibility of Pseudomonas aeruginosa strains from cystic fibrosis patients to bacteriophages. PLoS One 8, e60575. https://doi.org/10.1371/journal.pone.0060575.

Fister, S., Robben, C., Witte, A.K., Schoder, D., Wagner, M., Rossmanith, P., 2016. Influence of environmental factors on phage-bacteria interaction and on the efficacy and infectivity of phage P100. Front. Microbiol. 7, 1152. http://10.3389/fmicb.2016.01152.

Flint, R., Laucirica, D.R., Chan, H.K., Chang, B.J., Stick, S.M., Kicic, A., 2023. Stability considerations for bacteriophages in liquid formulations designed for nebulization. Cells 12, 10.3390/cells12162057.

Groulx, N.L.C., Turgeon, N., Volckens, J., Tremblay, M.E., Duchaine, C., 2016. Nanoscale aerovirology: an efficient yet simple method to analyze the viral distribution of single bioaerosols. Aerosol. Sci. Tech. 50, 732–739. http://doi.org/10.1080/02786826.2016.1184223.

Hac-Wydro, K.J.K., Dynarowicz-Łatka, P., 2009. Effect of saturation degree on the interactions between fatty acids and phosphatidylcholines in binary and ternary Langmuir monolayers. Colloids Surf B Biointerfaces 72, 101–111. http://10.1016/j.colsurfb.2009.03.019.

Hertel, S.P., Winter, G., Friess, W., 2015. Protein stability in pulmonary drug delivery via nebulization. Adv. Drug. Deliv. Rev. 93, 79–94. http://10.1016/j.addr.2014.10.003.
Israelachvili, J.N., 2011. Intermolecular and surface forces. 3rd ed. Academic Press, Burlington, MA.
Jiang, A.Y., Witten, J., Raji, I.O., Eweje, F., MacIsaac, C., Meng, S., Oladimeji, F.A., Hu, Y., Manan, R.S., Langer, R., Anderson, D.G., 2024. Combinatorial development of nebulized mRNA delivery formulations for the lungs. Nat. Nanotechnol. 19, 364–375. https://doi.org/10.1038/s41565-023-01548-3.
Le Guellec, S., Pardessus, J., Bodier-Montagutelli, E., L'Hostis, G., Dalloneau, E., Piel, D., Samai, H.C., Guillon, A., Mujic, E., Guillot-Combe, E., Ehrmann, S., Morello, E., Gabard, J., Heuze-Vourc'h, N., Fevre, C., Vecellio, L., 2023. Administration of bacteriophages via nebulization during mechanical ventilation: in vitro study and lung deposition in macaques. Viruses 15, 10.3390/v15030602.
Lee, H.W., Kharel, S., Loo, S.C.J., 2022. Lipid-coated hybrid nanoparticles for enhanced bacterial biofilm penetration and antibiofilm efficacy. ACS Omega 7, 35814-35824. http://10.1021/acsomega.2c04008.
Leung, S.S.Y., Carrigy, N.B., Vehring, R., Finlay, W.H., Morales, S., Carter, E.A., Britton, W.J., Kutter, E., Chan, H.K., 2019. Jet nebulization of bacteriophages with different tail morphologies - Structural effects. Int. J. Pharm. 554, 322-326. http://10.1016/j.ijpharm.2018.11.026.
Liu, K., Wen, Z., Li, N., Yang, W., Wang, J., Hu, L., Dong, X., Lu, J., Li, J., 2012. Impact of relative humidity and collection media on mycobacteriophage D29 aerosol. Appl. Environ. Microbiol. 78, 1466–1472. https://doi.org/10.1128/AEM.06610-11.
Liu, S., Wen, Y., Shan, X., Ma, X., Yang, C., Cheng, X., Zhao, Y., Li, J., Mi, S., Huo, H., Li, W., 2024. Charge-assisted stabilization of lipid nanoparticles enables inhaled mRNA delivery for mucosal vaccination. Nat. Commun. 15, 10.1038/s41467-024-53914-x.
Lokugamage, M.P., Vanover, D., Beyersdorf, J., Hatit, M.Z.C., Rotolo, L., Echeverri, E.S., Peck, H.E., Ni, H., Yoon, J.K., Kim, Y., Santangelo, P.J., Dahlman, J.E., 2021. Optimization of lipid nanoparticles for the delivery of nebulized therapeutic mRNA to the lungs. Nat Biomed. Eng. 5, 1059–1068. https://doi.org/10.1038/s41551-021-00786-x.
Malik, D.J., Sokolov, I.J., Vinner, G.K., Mancuso, F., Cinquerrui, S., Vladisavljevic, G.T., Clokie, M.R.J., Garton, N.J., Stapley, A.G.F., Kirpichnikova, A., 2017. Formulation, stabilisation and encapsulation of bacteriophage for phage therapy. Adv. Colloid Interface Sci. 249, 100-133. http://10.1016/j.cis.2017.05.014.
Meers, P., Neville, M., Malinin, V., Scotto, A.W., Sardaryan, G., Kurumunda, R., Mackinson, C., James, G., Fisher, S., Perkins, W.R., 2008. Biofilm penetration, triggered release and in vivo activity of inhaled liposomal amikacin in chronic Pseudomonas aeruginosa lung infections. J. Antimicrob. Chemother. 61, 859–868. http://10.1093/jac/dkn059.
Montefusco-Pereira, C.V., 2023. Steps toward nebulization in-use studies to understand the stability of new biological entities. Drug. Discov. Today 28, 103461. http://10.1016/j.drudis.2022.103461.
Morello, E.S.E., Maura, D., Huerre, M., Touqui, L., Debarbieux, L., 2011. Pulmonary delivery of bacteriophages targeting Pseudomonas aeruginosa: potential treatment of acute lung infections. PloS one 6, e16963. http://doi.org/10.1371/journal.pone.0016963.
Nap, R.J., Bozic, A.L., Szleifer, I., Podgornik, R., 2014. The role of solution conditions in the bacteriophage PP7 capsid charge regulation. Biophys. J. 107, 1970-1979. http://10.1016/j.bpj.2014.08.032.
Neary, M.T., Mulder, L.M., Kowalski, P.S., MacLoughlin, R., Crean, A.M., Ryan, K.B., 2024. Nebulised delivery of RNA formulations to the lungs: from aerosol to cytosol. J. Control Release 366, 812-833. http://10.1016/j.jconrel.2023.12.012.
Rosen, M.J., 2004. Surfactants and interfacial phenomena, 3rd ed. Wiley-Interscience, Hoboken, N.J.
Rudokas, M., Najlah, M., Alhnan, M.A., Elhissi, A., 2016. Liposome delivery systems for inhalation: a critical review highlighting formulation issues and anticancer applications. Med. Princ. Pract. 25 Suppl 2, 60–72. http://10.1159/000445116.
Saussereau, E., Vachier, I., Chiron, R., Godbert, B., Sermet, I., Dufour, N., Pirnay, J.P., De Vos, D., Carrie, F., Molinari, N., Debarbieux, L., 2014. Effectiveness of bacteriophages in the sputum of cystic fibrosis patients. Clin. Microbiol. Infect. 20, O983–O990. http://10.1111/1469-0691.12712.
Semler, D.D., Goudie, A.D., Finlay, W.H., Dennis, J.J., 2014. Aerosol phage therapy efficacy in Burkholderia cepacia complex respiratory infections. Antimicrob. Agents Chemother. 58, 4005–4013. https://doi.org/10.1128/AAC.02388-13.
Soto-Arriaza, M.A., Olivares-Ortega, C., Quina, F.H., Aguilar, L.F., Sotomayor, C.P., 2013. Effect of cholesterol content on the structural and dynamic membrane properties of DMPC/DSPC large unilamellar bilayers. Biochim Biophys Acta 1828, 2763–2769. http://10.1016/j.bbamem.2013.07.031.
Szabová, J.M.O., Havlíková, M., Lízal, F., Mravec, F., 2021. Influence of liposomes composition on their stability during the nebulization process by vibrating mesh nebulizer. Colloids Surf B Biointerfaces. http://10.1016/j.colsurfb.2021.111793.
Tai, K., He, X., Yuan, X., Meng, K., Gao, Y., Yuan, F., 2017. A comparison of physicochemical and functional properties of icaritin-loaded liposomes based on different surfactants. Colloids Surf A Physicochem Eng Asp 518, 218–231. https://doi.org/10.1016/j.colsurfa.2017.01.019.
Turgeon, N.T.M.J., Martel, B., Moineau, S., Duchaine, C., 2014. Comparison of five bacteriophages as models for viral aerosol studies. Appl. Environ. Microbiol. 80, 4242–4250. http://10.1128/AEM.00767-14.
Wang, D.Y., van der Mei, H.C., Ren, Y., Busscher, H.J., Shi, L., 2019. Lipid-based antimicrobial delivery-systems for the treatment of bacterial infections. Front Chem 7, 872. http://10.3389/fchem.2019.00872.
Wang, Y., Khanal, D., Chang, R.Y.K., Shang, X., Yang, H., Britton, W.J., Nelson, D., Chan, H.K., 2020. Can bacteriophage endolysins be nebulised for inhalation delivery against Streptococcus pneumoniae? Int. J. Pharm. 591. https://doi.org/10.1016/j.ijpharm.2020.119982.
Yan, W., Banerjee, P., Xu, M., Mukhopadhyay, S., Ip, M., Carrigy, N.B., Lechuga-Ballesteros, D., To, K.K.W., Leung, S.S.Y., 2021. Formulation strategies for bacteriophages to target intracellular bacterial pathogens. Adv. Drug. Deliv. Rev. 176, 113864. http://10.1016/j.addr.2021.113864.